All Inorganic Semiconductor Nanowire Mesh for Direct Solar Water Splitting

Bin Liu,*,†,∥ Cheng-Hao Wu,†,§ Jianwei Miao,∥ and Peidong Yang*,†,‡,§

†Department of Chemistry, University of California, Berkeley, California 94720, United States, ‡Department of Materials Science and Engineering, University of California, Berkeley, California 94720, United States, §Materials Sciences Division, Lawrence Berkeley National Laboratory, Berkeley, California 94720, United States, and ∥School of Chemical and Biomedical Engineering, Nanyang Technological University, Singapore 637459, Singapore

ABSTRACT The generation of chemical fuels *via* direct solar-to-fuel conversion from a fully integrated artificial photosynthetic system is an attractive approach for clean and sustainable energy, but so far there has yet to be a system that would have the acceptable efficiency, durability and can be manufactured at a reasonable cost. Here, we show that a semiconductor mesh made from all inorganic nanowires can achieve unassisted solar-driven, overall water-splitting without using any electron mediators. Free-standing nanowire mesh networks could be made in large scales using solution synthesis and vacuum filtration, making this approach attractive for low cost implementation.

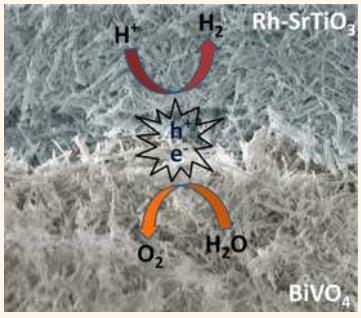

KEYWORDS: semiconductor nanowire · $BiVO_4$ · Rh-$SrTiO_3$ · artificial photosynthesis · solar water splitting

Photoelectrolysis of water using semiconductors as the light absorbing materials is one of the most intriguing ways to achieve clean and renewable energy systems.[1−4] Two photocatalytic systems for overall solar water-splitting, including a single light absorber system and a two-light absorber system, have been studied extensively.[5−14] Unfortunately, most of the semiconductors in a single light absorber system, which can satisfy both the energy and band edge requirements, are wide bandgap semiconductor oxides.[10,15] The intrinsic materials limitations associated with wide bandgap semiconductors limit photon absorption only to the ultraviolet portion of the solar spectrum. Development of photoelectrodes with visible light response has been actively pursued for efficient utilization of solar energy. It has been shown that GaP,[16,17] Fe_2O_3,[18,19] WO_3,[20] $BiVO_4$,[21,22] TaON,[23] Ta_3N_5,[24] Rh-$SrTiO_3$,[25,26] and $LaTiO_2N$[27] have visible activities for solar water-splitting; however, none of them can achieve hydrogen and oxygen evolution simultaneously.

In the 1970s, Nozik proposed an interesting idea of photochemical diodes for overall water-splitting.[28] The merit of the photochemical diode is to couple together a photocathode and a photoanode made of small bandgap semiconductors (which by themselves cannot achieve overall water-splitting) and utilize the combined photovoltages to drive the spontaneous solar water-splitting, so that a larger part of the solar spectrum can be used to achieve higher energy conversion efficiency. Later on, this idea was extended to semiconductor particulate photocatalyst system based on the z-scheme.[12,13,23,26,29] The z-scheme is composed of a hydrogen-evolving photocatalyst, an oxygen-evolving photocatalyst and an electron mediator for shuttling the photogenerated carriers between the hydrogen- and oxygen-evolving photocatalysts. However, the frequently used ionic electron mediators such as Fe^{2+}/Fe^{3+} and I^-/IO_3^- in z-scheme not only restricts the materials choices for photocatalysts, but also may cause undesired effects such as back reactions and undesirable light shielding.[29]

To develop an efficient solar water splitting system, it is necessary: (1) to develop semiconductor materials which absorb in the visible region of solar spectrum; (2) to design architectures for effective capture and conversion of sunlight, at the same time, allowing easy transport of protons and gas products; (3) to develop robust ion-conducting membranes, which are

* Address correspondence to liubin@ntu.edu.sg, p_yang@berkeley.edu.

Received for review September 14, 2014 and accepted November 3, 2014.

Published online November 03, 2014
10.1021/nn5051954

© 2014 American Chemical Society

impermeable to the gas products; and (4) to integrate each individual component into a complete and functioning system.[30]

In the present study, we developed a new architecture for direct solar water-splitting. In this design, semiconductor photocatalysts were synthesized as one-dimensional nanowires, which were assembled into free-standing, paper-like mesh for solar water-splitting. The large aspect ratio of semiconductor nanowires allows for the formation of intertwined and porous nanowire networks. The porous structure of nanowire mesh networks can benefit photochemical reactions by decoupling directions for light absorption and charge carrier extraction as well as providing a large area of catalytic surfaces. Furthermore, the porous structure can also facilitate proton transport and gas evolution. In our proof-of-concept experiments, we used $BiVO_4$ and Rh-$SrTiO_3$ nanowires for overall water-splitting, where $BiVO_4$ nanowires act as a photoanode for water oxidation and Rh-$SrTiO_3$ nanowires work as a photocathode for water reduction.

RESULTS AND DISCUSSION

To test the combination of materials for overall solar water-splitting, we first made two photoelectrodes of $BiVO_4$ and Rh-$SrTiO_3$ using sol−gel method followed by spin-coating on fluorine-doped SnO_2 (FTO) substrates (Methods). After loading the co-catalyst (CoO_x for $BiVO_4$ and Ru for Rh-$SrTiO_3$) on the surface of photoelectrodes, a photoelectrochemical cell consisting of a Rh-$SrTiO_3$ photocathode and a $BiVO_4$ photoanode was constructed. Photoelectrochemical water-splitting was carried out under visible light ($\lambda \geq$ 400 nm) in a sealed reactor without applying any external bias. Steady photocurrent was obtained, which agrees well with the evolution rate of hydrogen (Figure 1). The amount of hydrogen evolved was nearly twice as much as that of evolved oxygen and close to half amount of electrons which had passed through the external circuit, indicating the occurrence of self-driving photoelectrolysis of water. The estimated solar-to-fuel conversion efficiency is ~0.015%. Thus, the combination of $BiVO_4$ and Rh-$SrTiO_3$ can lead to spontaneous splitting of water to generate hydrogen and oxygen under visible light irradiation.

$SrTiO_3$ is a perovskite material with a cubic crystal structure. The necessity of breaking crystal symmetry makes direct synthesis of anisotropic Rh-$SrTiO_3$ nanowires difficult. In this study, we adopted a general self-templated ion exchange method for preparing Rh-$SrTiO_3$ and $BiVO_4$ nanowires in large scales for assembling nanowire mesh. This self-templated method involves two steps: growth of nanowire templates ($H_2Ti_3O_7$ nanowires for Rh-$SrTiO_3$ and $Na_2V_6O_{16}\cdot 3H_2O$ nanowires for $BiVO_4$, see Supporting Information Figure SI-1) and ion-exchange to convert nanowire templates to desired materials without damaging the

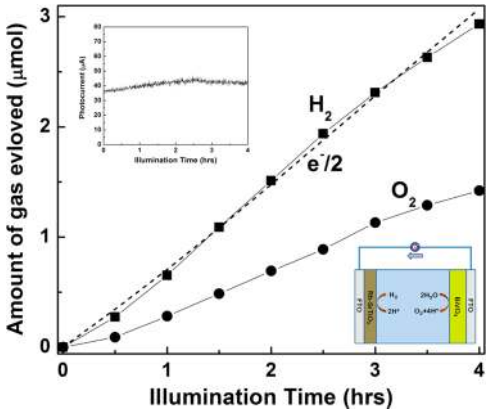

Figure 1. Photoelectrochemical overall water splitting over linked Rh-$SrTiO_3$ and $BiVO_4$ photoelectrodes without applying any external bias under visible light irradiation. Dashed line: half amount of electrons which had passed through the external circuit of linked photoelectrochemical cell; (■) hydrogen evolution rate and (●) oxygen evolution rate. Insets show photocurrent *versus* time of externally short-circuited Rh-$SrTiO_3$ and $BiVO_4$ photoelectrodes (left) and schematic of a Rh-$SrTiO_3$ and $BiVO_4$ photoelectrolysis cell system for overall solar-driven water splitting (right).

nanowire morphology. Figure 2a,b shows FESEM and TEM images of Rh-$SrTiO_3$ and $BiVO_4$ nanowires after ion-exchange. The nanowires have rough surfaces with mean diameters of 150 and 80 nm for Rh-$SrTiO_3$ and $BiVO_4$, respectively. The nanowires are phase-pure (Figure 2c) with no detectable sodium after ion-exchange by energy dispersive X-ray spectroscopy (EDX). The rhodium was introduced into $SrTiO_3$ during the ion-exchange process, which shifts the light absorption onset of $SrTiO_3$ from UV to visible. The absorption onsets of Rh-$SrTiO_3$ and $BiVO_4$ nanowires were estimated to be ~700 and ~510 nm from the diffuse reflectance spectra as shown in Figure 2d. As shown in Supporting Information Figures SI-2 and SI-3, high-resolution transmission electron microscopy (HRTEM) analysis was further performed to examine the crystal quality of Rh-$SrTiO_3$ and $BiVO_4$ nanowires. The HRTEM images reveal the interplanar spacing of 0.276 nm (Supporting Information Figure SI-3a) and 0.255 nm (Supporting Information Figure SI-3b), corresponding to the (110) crystal plane of $SrTiO_3$ and the (002) crystal plane of monoclinic $BiVO_4$.

The Rh-$SrTiO_3$ and $BiVO_4$ nanowires exhibited stable photocatalytic activity in the production of hydrogen and oxygen from water under visible light irradiation (Supporting Information). Hydrogen and oxygen gas evolution as a function of time during a 7-h testing period is shown in Supporting Information Figure SI-4. The hydrogen and oxygen production rate is ~0.26 μmol hour^{-1} based on 2 mg of Rh-$SrTiO_3$ nanowires loaded with 1 wt % Ru and ~0.41 μmol h^{-1} based on 2 mg of $BiVO_4$ nanowires, respectively. The measurements were carried out in a quartz container filled with 1:1 water −methanol solution for the evolution of hydrogen (methanol is used as the hole scavenger) or $Fe_2(SO_4)_3$

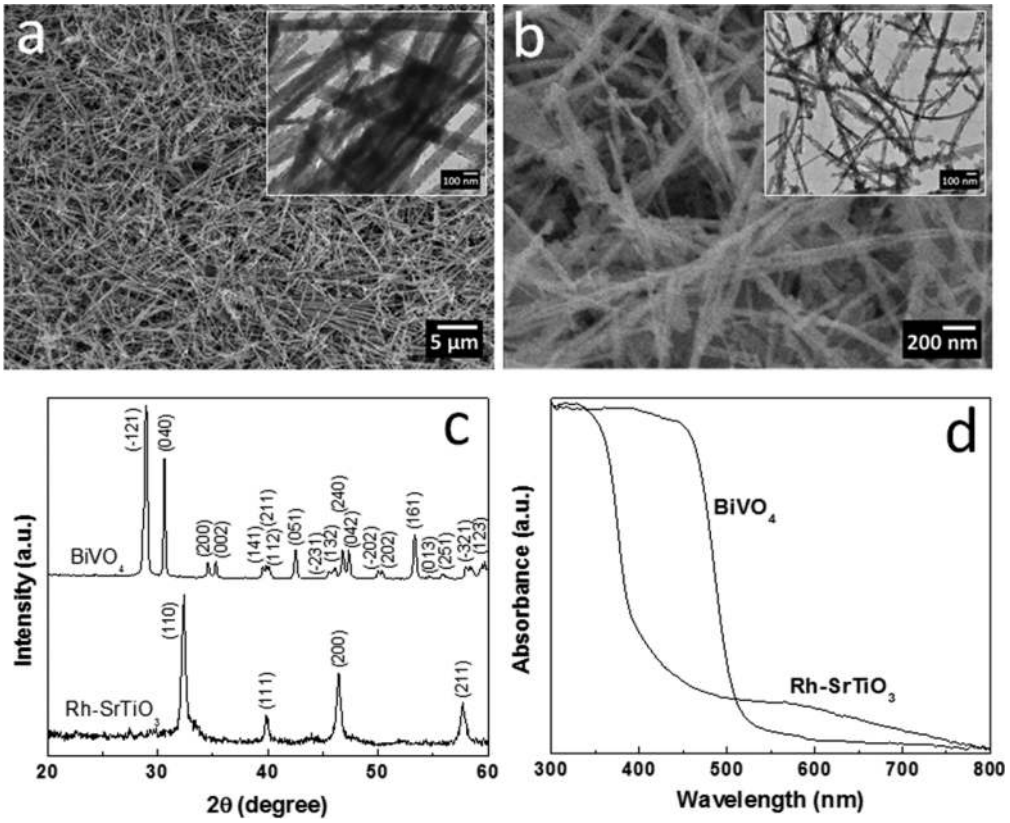

Figure 2. $Rh\text{-}SrTiO_3$ and $BiVO_4$ nanowires. (a and b) FESEM and TEM images of $Rh\text{-}SrTiO_3$ and $BiVO_4$ nanowires, respectively. (c) XRD patterns of $Rh\text{-}SrTiO_3$ and $BiVO_4$ nanowires. (d) UV−vis absorption spectra of $Rh\text{-}SrTiO_3$ and $BiVO_4$ nanowires showing the absorption onsets.

aqueous solution for the evolution of oxygen (Fe^{3+} is used as the electron scavenger).

After 1 wt % Ru co-catalyst was loaded on the surface of $Rh\text{-}SrTiO_3$ nanowires, the $Ru/Rh\text{-}SrTiO_3$ and $BiVO_4$ nanowires were assembled into nanowire meshes using vacuum filtration. The reason for selecting Ru as the co-catalyst instead of Pt is that Ru is an effective co-catalyst for hydrogen evolution that does not enhance back reaction for water formation from evolved H_2 and O_2.[25] Two types of nanowire mesh films were assembled including mixed $Ru/Rh\text{-}SrTiO_3$ and $BiVO_4$ nanowire mesh film and bilayer $Ru/Rh\text{-}SrTiO_3$ and $BiVO_4$ nanowire mesh film (Figure 3, Supporting Information Figures SI-6−SI-8). Prior to photoelectrochemical testing, the nanowire mesh films were annealed at 500−800 °C in argon to promote good contact between the $Ru/Rh\text{-}SrTiO_3$ and $BiVO_4$ nanowires.

The nanowire mesh film was tested for overall water-splitting by immersing it in deionized water with visible light irradiation ($\lambda \geq 400$ nm). Overall water-splitting into H_2 and O_2 in a stoichiometric ratio proceeded on $Ru/Rh\text{-}SrTiO_3$ and $BiVO_4$ nanowire mesh film without using any electron mediator. Figure 4a shows the stoichiometric evolution of H_2 and O_2 on a mixed nanowire mesh film under visible light irradiation, and there was almost no degradation of activity in three repeated runs within 18 h. The total evolved H_2 and O_2 was ~4.5 μmol, corresponding to an overall solar-to-fuel conversion efficiency of 0.0017%. The turnover number of reacted electrons to the total number of Rh in $Rh\text{-}SrTiO_3$ was estimated to be ~7.4. The photoactivity depended on the relative amount of $Ru/Rh\text{-}SrTiO_3$ to $BiVO_4$. The highest photoactivity was obtained using mixed nanowire mesh film assembled from equal amounts of $Ru/Rh\text{-}SrTiO_3$ and $BiVO_4$ nanowires. If $Ru/Rh\text{-}SrTiO_3$ nanowires alone were tested under visible light, only trace amount of H_2 could be produced (Supporting Information Figure SI-5). On the other hand, if $BiVO_4$ nanowires were tested alone, almost no gas product was observed (Supporting Information Figure SI-5), suggesting the importance of $Ru/Rh\text{-}SrTiO_3$−$BiVO_4$ interface for overall water-splitting. Since the conduction band of $BiVO_4$ is more positive than H^+/H_2 reduction potential, $BiVO_4$ itself cannot achieve overall water-splitting as photogenerated electrons in $BiVO_4$ do not have sufficient energy to reduce proton. However, when coupled with $Ru/Rh\text{-}SrTiO_3$, a two-photon z-scheme configuration could be constructed. In this case, the minority carriers in each semiconductor participate in chemical reactions, while the majority carriers recombine at the heterojunction interface (Supporting Information Figure SI-9).

The ultimate goal of applying the nanowire mesh design in solar water-splitting is to achieve simultaneous

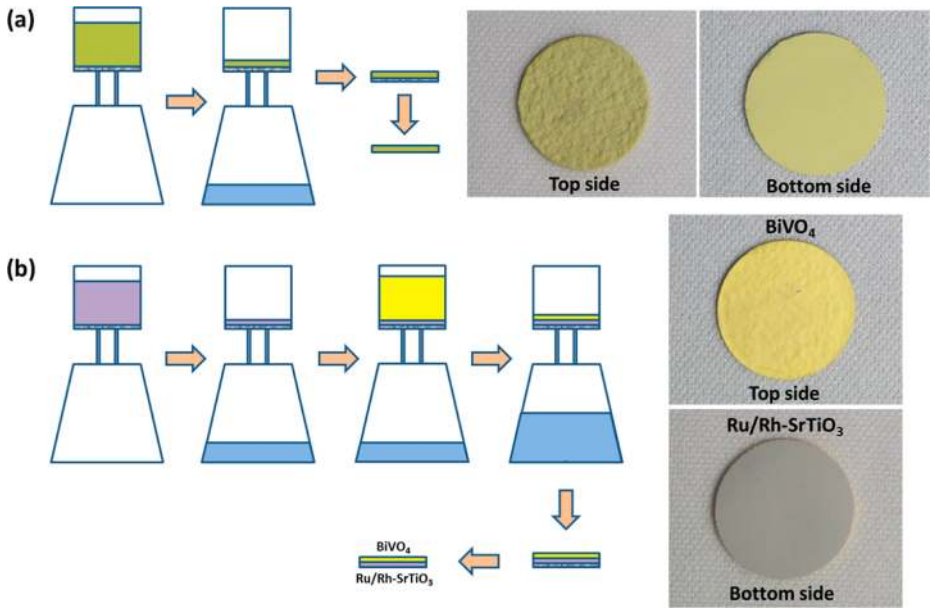

Figure 3. Formation of mixed and bilayer Ru/Rh-$SrTiO_3$ and $BiVO_4$ nanowire mesh. (a and b) Schematic illustrations of formation of mixed and bilayer Ru/Rh-$SrTiO_3$ and $BiVO_4$ nanowire mesh films.

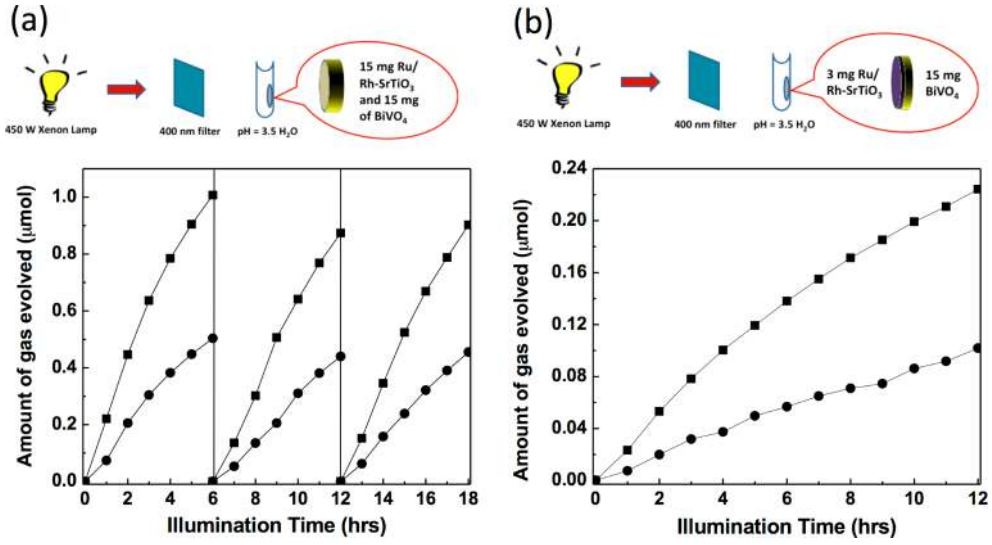

Figure 4. Overall water-splitting under visible light irradiation. (a) Cycling measurements of hydrogen (■) and oxygen (●) evolution from overall photocatalytic water splitting using mixed Ru/Rh-$SrTiO_3$ and $BiVO_4$ nanowire mesh film. (b) Overall water splitting into hydrogen (■) and oxygen (●) using bilayer Ru/Rh-$SrTiO_3$ and $BiVO_4$ nanowire mesh film.

production and separation of H_2 and O_2, which is possible if a bilayer nanowire mesh is employed. Figure 4b shows the evolution of H_2 and O_2 on a bilayer nanowire mesh film assembled from 3 mg of Ru/Rh-$SrTiO_3$ nanowires and 15 mg of $BiVO_4$ nanowires and irradiated from Ru/Rh-$SrTiO_3$ nanowire side. Stoichiometric evolution of H_2 and O_2 was evident from the beginning of the reaction. The evolution rate of H_2 and O_2 decreased if more than or less than 3 mg of Ru/Rh-$SrTiO_3$ nanowires were used while fixing $BiVO_4$ nanowires at 15 mg. This result indicated the importance of both Ru/Rh-$SrTiO_3$−$BiVO_4$ interface and the balance in light absorption by each photocatalyst in a two-photon system (3 mg of Ru/Rh-$SrTiO_3$ nanowires form a porous nanowire mesh with a thickness of ~2 μm, which is much smaller than the light absorption depth of Ru/Rh-$SrTiO_3$ (~20 μm). Thus, if light is illuminated from Ru/Rh-$SrTiO_3$ nanowire mesh side with 3 mg of Ru/Rh-$SrTiO_3$ nanowires, a significant amount of photons with energy greater than the bandgap of $BiVO_4$ can bypass the Ru/Rh-$SrTiO_3$ nanowire mesh film, reach $BiVO_4$ nanowires, and be absorbed by $BiVO_4$ nanowires). The optimized evolution rate of H_2 or O_2 for a bilayer nanowire mesh was only one-eighth of the optimized value for a mixed nanowire mesh. The lower photoactivity was due to the less physical contact

among nanowires in a bilayer nanowire mesh film, resulting in poorer charge separation. Thus, mixing nanowires together with conductive additives such as metallic carbon nanotubes or graphene sheets during the preparation of bilayer films might lead to enhancement in the production of H_2 and O_2.[31]

CONCLUSION

In conclusion, we have demonstrated a two-light absorber architecture for spontaneous overall water-splitting based on the concept of nanowire meshes. These free-standing nanowire mesh networks could be made in large scales using vacuum filtration, a process used industrially to make paper, making them attractive for low cost implementation. Overall, water-splitting without using the electron mediators was observed for both mixed and bilayer nanowire mesh films. The bilayer film based on semiconductor nanowires can be a promising candidate for the artificial photosynthetic system.

METHODS

Preparation of $BiVO_4$ Photoanode. A total of 0.97 g of $Bi(NO_3)_3 \cdot 5H_2O$ (Sigma-Aldrich; 98%) and 0.23 g of NH_4VO_3 (Sigma-Aldrich; 99%) were dissolved in 10 mL of 2 mol/L HNO_3 solution to form a yellow precursor solution. A piece of FTO substrate (F:SnO_2, Tec 15, 10 Ω/□, Hartford Glass Company) was dipped in the precursor solution for 5 s, followed by slowly pulling the substrate out. Then, the FTO substrate was covered with a thin layer of yellow liquid. After it was dried at room temperature, the FTO substrate covered with an orange film was calcined at 400 °C in air for 2 h for the preparation of $BiVO_4$ film. Cobalt oxide cocatalyst was loaded on the $BiVO_4$ film by an impregnation method followed by calcination at 400 °C in air for 1 h. The impregnation solution was 80 mmol/L $Co(NO_3)_2$ aqueous solution.

Preparation of Rh-$SrTiO_3$ Photocathode. First, 1.06 g of $SrCl_2 \cdot 6H_2O$ (Sigma-Aldrich; 99%) was dissolved in 35 mL of ethanol, followed by adding 0.82 mL of acetylacetone ($C_5H_8O_2$). After the solution stirred for 30 min, 1.19 mL of titanium isopropoxide ($Ti(OCH(CH_3)_2)_4$, Sigma-Aldrich; 97%) and 11.5 mg of $Rh(NO_3)_3 \cdot nH_2O$ were added into the solution and the solution was vigorously stirred for another 30 min. The molar ratio of the mixture of $SrCl_2 \cdot 6H_2O/C_5H_8O_2/Rh(NO_3)_3 \cdot nH_2O/Ti(OCH(CH_3)_2)_4$ was 1:2:1:0.01. The mixed solution was then hydrolyzed by adding 5 mL of 0.1 mol/L HCl solution, and subjected to vigorous stirring for 10 min at room temperature. Finally, 5 mL of polyethylene glycol 200 was added to yield the coating solution. Rh-$SrTiO_3$ film was spin-casted onto FTO substrates followed by calcination at 500 °C for 1 h in air. Ru co-catalyst was loaded on the Rh-$SrTiO_3$ film by photodeposition from an aqueous-methanol solution (10 vol % methanol) containing $RuCl_3 \cdot nH_2O$.

Rh-$SrTiO_3$ Nanowire Synthesis. Six grams of anatase nanopowder (average size: 25−70 nm, Aldrich) was mixed with 50 mL of NaOH aqueous solution (15 M) at room temperature. The mixture was heated in a 125 mL Teflon-lined autoclave (Parr Instrument Co.) at 180 °C for 3 days. After the hydrothermal synthesis, the precipitates were collected and washed extensively with 0.6 M HCl aqueous solution and water to exchange Na^+ with H^+ for the synthesis of $H_2Ti_3O_7$ nanowires. Rh-$SrTiO_3$ nanowires were synthesized from a solvothermal ion-exchange reaction using $H_2Ti_3O_7$ nanowires as the templates. 1.03 g of $H_2Ti_3O_7$ (4 mmol) nanowires were dispersed in 40 mL of 0.45 M $Sr(OH)_2$ aqueous-ethanol solution ($V_{ethanol}/V_{water}$ = 4:1), with a fixed strontium to titanium molar ratio of 1.5. Following, 1 mol % (Rh/Ti = 1/99) of $Rh(NO_3)_3$ was added into the suspension and the mixture was autoclaved in a 45 mL Teflon-lined autoclave (Parr Instrument Co.) at 120 °C for 2 days. After completion of the reaction, the harvested precipitates were washed repeatedly with 0.1 M formic acid to remove residue $SrCO_3$ and water, and dried in ambient air. The final products were calcined at 800 °C for 4 h.

$BiVO_4$ Nanowire Synthesis. One millimole of V_2O_5 power and 2 mmol of Na_2SO_4 were mixed in 30 mL of deionized water at room temperature. The mixture was heated in a 45 mL Teflon-lined autoclave at 180 °C for 24 h for the synthesis of $Na_2V_6O_{16} \cdot 3H_2O$ nanowire templates.[1] Subsequently, 132 mg of $Na_2V_6O_{16} \cdot 3H_2O$ (0.2 mmol) nanowires was mixed with 582 mg of $Bi(NO_3)_3 \cdot 5H_2O$ (1.2 mmol) in 40 mL of ethanol−water solution ($V_{ethanol}/V_{water}$ = 4:1). The mixture was autoclaved in a 45 mL Teflon-lined autoclave at 120 °C for 24 h to convert $Na_2V_6O_{16} \cdot 3H_2O$ nanowires into monoclinic $BiVO_4$ nanowires.

Nanowire Characterization. The crystal structure of the as-synthesized nanowires was examined by X-ray diffraction (XRD, Bruker D8 X-ray diffractometer D71). Morphological and lattice structural information were examined with field emission scanning electron microscopy (FESEM, JSM-6340F), transmission electron microscopy, selected area electron diffraction, and energy dispersive X-ray spectroscopy (TEM/SAED/EDX, Hitachi H-7650). The optical absorption spectra were recorded using a UV−vis-NIR scanning spectrophotometer equipped with an integration sphere (Shimadzu UV-3101PC).

Co-Catalyst Loading. Ru co-catalysts (1 wt %), working as active sites for hydrogen evolution, were loaded on Rh-$SrTiO_3$ nanowires (367 mg) by photodeposition in an aqueous-methanol solution (50 mL, 10 vol % methanol) containing $RuCl_3 \cdot nH_2O$ (7.26 mM). The Ru-loaded Rh-$SrTiO_3$ nanowires were harvested by filtration and washed with deionized water and dried in ambient air.

Nanowire Mesh Fabrication. The nanowire mesh networks were assembled by filtration of a nanowire suspension onto a filter membrane. For example, to fabricate bilayer Ru/Rh-$SrTiO_3$ and $BiVO_4$ nanowire mesh films, Ru/Rh-$SrTiO_3$ and $BiVO_4$ nanowires were first suspended in deionized water in two separate containers. The $BiVO_4$ nanowire suspension was filtered on a vacuum-filtration setup using PVDF filter membrane (Durapore, 0.5 μm pore size), followed by filtering the Ru/Rh-$SrTiO_3$ nanowire suspension. After filtration, the films on the filter membrane were allowed to dry in ambient air. Once completely dried, the nanowire mesh films could be detached from the filter membrane as free-standing discs. To promote good physical contact between Ru/Rh-$SrTiO_3$ and $BiVO_4$ nanowires, the nanowire mesh films were annealed at 500−800 °C in argon.

Photocatalytic Activity of Rh-$SrTiO_3$ and $BiVO_4$ Nanowires. Photocurrent of linked photoelectrochemical cell system was measured in a two-electrode cell without applying any external bias in a sealed Teflon reactor with a quartz window on its side wall for illumination. A 1 M NaOH aqueous solution was used as the electrolyte. The illumination was from a 300 W Xe lamp which passes through a long-pass filter with cutoff at 400 nm. During photochemical reactions, photocurrent and amounts of gas products were measured using a potentiostat (Electrochemical Workstation Zive SP2) and an inline gas chromatography (Agilent 490 MicroGC). The photocatalytic activity of the nanowire mesh films was evaluated using inline gas chromatography (Agilent 3000 MicroGC, MS-5A column, TCD, Ar carrier). The nanowire mesh film was suspended in pH = 3.5 deionized water (adjusted using dilute H_2SO_4) inside a side-window cell made of quartz, which is connected to a gas-closed circulation system. The solution was evacuated to remove dissolved air and purged with Ar before irradiation. The light source was a 450 W Xe lamp with a long-pass filter ($\lambda \geq 400$ nm) sitting in between the light source and the quartz reactor. The amounts of evolved gases were periodically determined with an inline gas chromatography.

Photocatalytic Activity of Rh-$SrTiO_3$ and $BiVO_4$ Nanowires. Rh-$SrTiO_3$ and $BiVO_4$ nanowires were tested for the production of hydrogen and oxygen from water under visible light irradiation, respectively. Photocatalytic reaction was carried out in a gas-closed circulation system. For the hydrogen evolution reaction, 2 mg of Rh-$SrTiO_3$ nanowires loaded with 1 wt % Ru was dispersed in 3 mL of water−methanol solution (50 vol % methanol) in a 14 mL quartz cell. For the oxygen evolution reaction, 2 mg of $BiVO_4$ nanowires was dispersed in 3 mL of $Fe_2(SO_4)_3$ aqueous solution (total 6 mg of $Fe_2(SO_4)_3 \cdot xH_2O$) in a 14 mL quartz cell. Argon (~1300 Torr) was introduced into the reaction system after deaeration. The reaction system was irradiated using a 450 W Xe lamp with a long-pass cutoff filter (λ = 400 nm). The amount of evolved gas was determined every 1 h using an inline gas chromatography (Agilent 3000A Micro GC).

Conflict of Interest: The authors declare no competing financial interest.

Supporting Information Available: FESEM, TEM, HRTEM, XRD, UV−vis and photoactivity measurements. This material is available free of charge via the Internet at http://pubs.acs.org.

Acknowledgment. This work was supported by the Director, Office of Science, Office of Basic Energy Sciences, Materials Sciences and Engineering Division, of the U.S. Department of Energy under Contract No. DE-AC02-05CH11231(P-Chem) and the **Sin**gapore-**Ber**keley **R**esearch **I**nitiative for **S**ustainable **E**nergy (**SinBeRISE**). These authors thank C. K. Chan, C. Liu, and J. W. Sun for helpful discussions.

REFERENCES AND NOTES

1. Kamat, P. V. Meeting the Clean Energy Demand: Nanostructure Architectures for Solar Energy Conversion. *J. Phys. Chem. C* **2007**, *111*, 2834–2860.
2. Hagfeldt, A.; Gratzel, M. Light-Induced Redox Reactions in Nanocrystalline Systems. *Chem. Rev.* **1995**, *95*, 49–68.
3. van de Krol, R.; Liang, Y. Q.; Schoonman, J. Solar Hydrogen Production with Nanostructured Metal Oxides. *J. Mater. Chem.* **2008**, *18*, 2311–2320.
4. Osterloh, F. E. Inorganic Nanostructures for Photoelectrochemical and Photocatalytic Water Splitting. *Chem. Soc. Rev.* **2013**, *42*, 2294–2320.
5. Bard, A. J.; Fox, M. A. Artificial Photosynthesis: Solar Splitting of Water to Hydrogen and Oxygen. *Acc. Chem. Res.* **1995**, *28*, 141–145.
6. Fujishima, A.; Zhang, X. T.; Tryk, D. A. TiO_2 Photocatalysis and Related Surface Phenomena. *Surf. Sci. Rep.* **2008**, *63*, 515–582.
7. Kudo, A.; Miseki, Y. Heterogeneous Photocatalyst Materials for Water Splitting. *Chem. Soc. Rev.* **2009**, *38*, 253–278.
8. Khan, S. U. M.; Al-Shahry, M.; Ingler, W. B. Efficient Photochemical Water Splitting by a Chemically Modified n-TiO_2. *Science* **2002**, *297*, 2243–2245.
9. Zou, Z. G.; Ye, J. H.; Sayama, K.; Arakawa, H. Direct Splitting of Water Under Visible Light Irradiation with an Oxide Semiconductor Photocatalyst. *Nature* **2001**, *414*, 625–627.
10. Kato, H.; Asakura, K.; Kudo, A. Highly Efficient Water Splitting into H_2 and O_2 over Lanthanum-Doped $NaTaO_3$ Photocatalysts with High Crystallinity and Surface Nanostructure. *J. Am. Chem. Soc.* **2003**, *125*, 3082–3089.
11. Maeda, K.; Teramura, K.; Lu, D. L.; Takata, T.; Saito, N.; Inoue, Y.; Domen, K. Photocatalyst Releasing Hydrogen from Water. *Nature* **2006**, *440*, 295–295.
12. Kato, H.; Hori, M.; Konta, R.; Shimodaira, Y.; Kudo, A. Construction of Z-scheme Type Heterogeneous Photocatalysis Systems for Water Splitting into H_2 and O_2 Under Visible Light Irradiation. *Chem. Lett.* **2004**, *33*, 1348–1349.
13. Abe, R.; Sayama, K.; Sugihara, H. Development of New Photocatalytic Water Splitting into H_2 and O_2 Using Two Different Semiconductor Photocatalysts and a Shuttle Redox Mediator IO_3^-/I^-. *J. Phys. Chem. B* **2005**, *109*, 16052–16061.
14. Maeda, K.; Higashi, M.; Lu, D. L.; Abe, R.; Domen, K. Efficient Nonsacrificial Water Splitting through Two-Step Photoexcitation by Visible Light Using a Modified Oxynitride as a Hydrogen Evolution Photocatalyst. *J. Am. Chem. Soc.* **2010**, *132*, 5858–5868.
15. Fujishima, A.; Honda, K. Electrochemical Photolysis of Water at a Semiconductor Electrode. *Nature* **1972**, *238*, 37–38.
16. Ohashi, K.; McCann, J.; Bockris, J. O. M. Stable Photoelectrochemical Cells for the Splitting of Water. *Nature* **1977**, *266*, 610–611.
17. Sun, J. W.; Liu, C.; Yang, P. D. Surfactant-Free, Large-Scale, Solution-Liquid-Solid Growth of Gallium Phosphide Nanowires and Their Use for Visible-Light-Driven Hydrogen Production from Water Reduction. *J. Am. Chem. Soc.* **2011**, *133*, 19306–19309.
18. Cesar, I.; Kay, A.; Martinez, J. A. G.; Gratzel, M. Translucent Thin Film Fe_2O_3 Photoanodes for Efficient Water Splitting by Sunlight: Nanostructure-Directing Effect of Si-Doping. *J. Am. Chem. Soc.* **2006**, *128*, 4582–4583.
19. Gao, H. W.; Liu, C.; Jeong, H. E.; Yang, P. D. Plasmon-Enhanced Photocatalytic Activity of Iron Oxide on Gold Nanopillars. *ACS Nano* **2012**, *6*, 234–240.
20. Santato, C.; Odziemkowski, M.; Ulmann, M.; Augustynski, J. Crystallographically Oriented Mesoporous WO_3 Films: Synthesis, Characterization, and Applications. *J. Am. Chem. Soc.* **2001**, *123*, 10639–10649.
21. Kudo, A.; Omori, K.; Kato, H. A Novel Aqueous Process for Preparation of Crystal Form-Controlled and Highly Crystalline $BiVO_4$ Powder from Layered Vanadates at Room Temperature and Its Photocatalytic and Photophysical Properties. *J. Am. Chem. Soc.* **1999**, *121*, 11459–11467.
22. Jia, Q.; Iwashina, K.; Kudo, A. Facile Fabrication of an Efficient $BiVO_4$ Thin Film Electrode for Water Splitting Under Visible Light Irradiation. *Proc. Natl. Acad. Sci. U.S.A.* **2012**, *109*, 11564–9.
23. Abe, R.; Higashi, M.; Domen, K. Facile Fabrication of an Efficient Oxynitride TaON Photoanode for Overall Water Splitting into H_2 and O_2 under Visible Light Irradiation. *J. Am. Chem. Soc.* **2010**, *132*, 11828–11829.
24. Higashi, M.; Domen, K.; Abe, R. Fabrication of Efficient TaON and Ta_3N_5 Photoanodes for Water Splitting Under Visible Light Irradiation. *Energy Environ. Sci.* **2011**, *4*, 4138–4147.
25. Konta, R.; Ishii, T.; Kato, H.; Kudo, A. Photocatalytic Activities of Noble Metal Ion Doped $SrTiO_3$ under Visible Light Irradiation. *J. Phys. Chem. B* **2004**, *108*, 8992–8995.
26. Iwashina, K.; Kudo, A. Rh-Doped $SrTiO_3$ Photocatalyst Electrode Showing Cathodic Photocurrent for Water Splitting under Visible-Light Irradiation. *J. Am. Chem. Soc.* **2011**, *133*, 13272–13275.
27. Zhang, F. X.; Yamakata, A.; Maeda, K.; Moriya, Y.; Takata, T.; Kubota, J.; Teshima, K.; Oishi, S.; Domen, K. Cobalt-Modified Porous Single-Crystalline $LaTiO_2N$ for Highly Efficient Water Oxidation under Visible Light. *J. Am. Chem. Soc.* **2012**, *134*, 8348–8351.
28. Nozik, A. J. Photochemical Diodes. *Appl. Phys. Lett.* **1977**, *30*, 567–569.
29. Sasaki, Y.; Nemoto, H.; Saito, K.; Kudo, A. Solar Water Splitting Using Powdered Photocatalysts Driven by Z-Schematic Interparticle Electron Transfer without an Electron Mediator. *J. Phys. Chem. C* **2009**, *113*, 17536–17542.
30. Yang, P. D.; Tarascon, J. M. Towards Systems Materials Engineering. *Nat. Mater.* **2012**, *11*, 560–563.
31. Iwase, A.; Ng, Y. H.; Ishiguro, Y.; Kudo, A.; Amal, R. Reduced Graphene Oxide as a Solid-State Electron Mediator in Z-Scheme Photocatalytic Water Splitting under Visible Light. *J. Am. Chem. Soc.* **2011**, *133*, 11054–11057.